Natural Hazards (2018) 94:1391–1413
https://doi.org/10.1007/s11069-018-3483-9

ORIGINAL PAPER

Effect of rainfall on the triggering of the devastating slope failure at Malin, India

Nabarun Dey[1] · Aniruddha Sengupta[1]

Received: 23 August 2017 / Accepted: 14 September 2018 / Published online: 21 September 2018

Abstract
A study on a devastating rainfall-induced landslide at Malin, India, which resulted in 160 deaths including the destruction of an entire village in July 2014 has been presented. The area was under a massive rainstorm which lasted for 3 days before the tragedy. The seepage into the slope due to the rainfall infiltration and the corresponding factor of safety of the slope at Malin has been quantified using a two-dimensional numerical model. The study indicates that the continuous rainfall infiltration develops a perched water table near the slope surface which results in the saturation and the positive pore water pressure build up at a shallow depth. With the increasing intensity and the rainfall duration, this depth of saturated zone increases rapidly. Though the Malin slope has an adequate factor of safety of 1.6, initially, but with continuous rainfall and increase in rainfall intensity, the factor of safety reduces to less than one on the day of tragedy. The parametric study indicates that the factor of safety of the Malin slope is adequate after 24 h of 2 mm/h, 5 mm/h and 10 mm/h of rainfall. But it drops rapidly to less than 1 after 7, 6, 6, 3, 2 and 1-h of 20 mm/h, 30 mm/h, 40 mm/h, 50 mm/h, 60 mm/h and 70 mm/h of rainfall, respectively. The slope, on which the Malin village is located, is initially safe but the debris from the upper portions of the slope moves downward destroying the residential area of the Malin village.

Keywords Landslide · Rainfall infiltration · Seepage · Slope failure · Factor of safety

1 Introduction

Rainfall-induced slope failures are very common in many parts of the world and depending upon the location; it often leads to significant damages to both human life and property. There are plenty of examples (Brown et al. 1982; Van Sint Jan and Talloni 1993; Schuster et al. 2002; Lagmay et al. 2006; Sengupta et al. 2010) available on large-scale destructive landslides in countries such as, China, Chile, India, Japan, Venezuela which are triggered

✉ Nabarun Dey
nabarun@iitkgp.ac.in

Aniruddha Sengupta
sengupta@civil.iitkgp.ernet.in

[1] Department of Civil Engineering, Indian Institute of Technology Kharagpur, Kharagpur 721302, India

by rainfall. It has been calculated that every year, on an average, the damage caused by landslides during a monsoon season costs more than one billion US dollar and around 200 fatalities (Naithani 1999).

Heavy rainfall along with hot and humid climatic conditions results in the formation of residual soils which generally exist in unsaturated conditions because of the low ground water table (Rahardjo et al. 1995). In an unsaturated soil, the initial suction pressures contribute to an increase in the shear strength of the soil. But with the increasing moisture content, the suction pressures start to decrease. When the soil becomes fully saturated, the suction pressures become zero and thereafter positive pore water pressures start to develop. The increase in the degree of saturation and consequently decrease in the matric suction, because of rain water infiltration, causes decrease in the shear strength of the unsaturated soils (Bishop 1959; Wilson and Dietrich 1987; Borja and White 2010). The matric suction has been found to be the most important parameter in the stability of unsaturated soil slopes (Fredlund and Rahardjo 1993) and its reduction often leads to the failure of a stable slope. The development of slip surfaces in a soil slope mainly depends on the slope inclination, soil properties, depth of residual soils, intensity and duration of rainfall. Since the amount of mass movement during a hill slope failure, in the form of debris, is huge, it can cause a serious disaster to both life and property. Thus, a clear physical understanding about the stability of a hill slope with varying rainfall infiltration is essential.

In the present study, a rainfall-induced hill slope failure which occurred in the Malin village near Mumbai in the state of Maharashtra, India, is the main focus. The tragedy happened on July 30, 2014, claiming about 160 lives including the burial of the whole village (refer to Fig. 1) having 44 houses and one primary school under the debris. A number of researchers (Ering et al. 2015; Meshram 2016; Naykodi et al. 2016) have looked into the Malin landslide in the recent past. Ering et al. (2015) back calculated the shear parameters of the Malin soils by limit equilibrium method, assuming that the slope was saturated and on the verge of failure with a factor of safety equal to one. They concluded that there had been a significant decrease in the shear strengths due to the rainfall infiltration into the slope. Meshram (2016) also looked into the factors that had direct impact on the Malin slope stability and reviewed some of the remedial measures to prevent such kind of disasters.

The present study attempts to recreate the tragedy of the Malin village by considering the Malin slope to be in unsaturated condition initially, generation of positive pore water pressures, matric suction reduction in soil slope with rainfall intensity and duration, the effect of the ground water table and day-by-day reduction of the safety factor of Malin hill slope. The published data on the Malin's soil properties, geological conditions, and the rainfall data are obtained from the literature (Ering et al. 2015; Meshram 2016). The reduction of the factor of safety for sliding failure of Malin's slope is determined for 2 mm/h, 5 mm/h, 10 mm/h, 20 mm/h, 30 mm/h, 40 mm/h, 50 mm/h, 60 mm/h and 70 mm/h intensity of rainfall with the results recorded at every 1-h interval. The stability of Malin slope has also been determined on day-by-day basis from 21st July, 2014 to 30th July, 2014 under different intensities of rainfall.

2 Site characterisation

The Malin village is located in Pune district in the state of Maharashtra, India. The geographical coordinate of the village is given by latitude N19°09′34″ and longitude E73°41′19″. The village is located at an altitude of 760 m above mean sea level and 110 km away from Mumbai (refer to Fig. 2).

(a)

(b)

Fig. 1 Malin village **a** before, and **b** after landslide (BBC News, 30 July 2014)

The top surface of Malin slope is weathered basalt and classified as silty clay with loose gravels. The colour of the rock is dark grey, while the surface material is grey to red. The slope of the Malin hill is more or less uniform and gentle to moderate in nature. The entire hill slopes may be divided into four zones depending upon their inclination. A small stream (locally called 'nala') is located at the foothill of Malin. The Zone 1 is located between the main road of Malin village and the stream. The slope is relatively flatter near the stream. The upper portion of Zone 1, that is, the slope below the main road has a gentle slope with an average inclination of 20°. The lower part of Zone 2, where the main road and 46 houses are located has a very gentle slope of 10°. The upper part of Zone 2 has an average inclination of 25°. The Zone 3 has an average inclination of 30°. The lower part of Zone 4 is basically agricultural field with a varying inclination of 15°–25°. The upper part of Zone

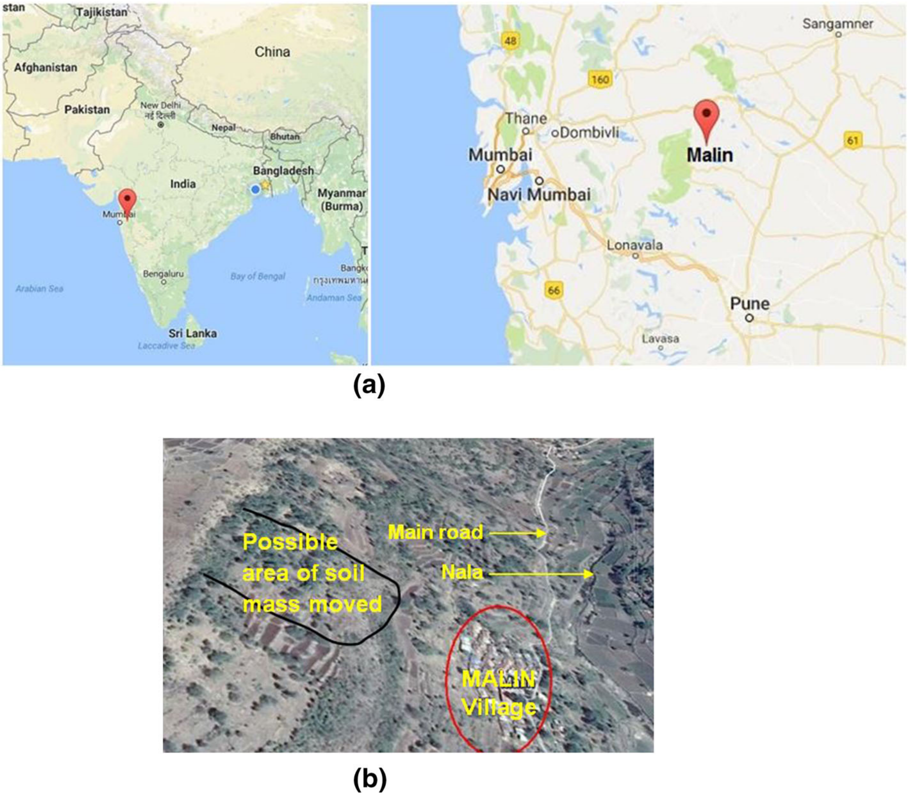

Fig. 2 **a** Location of Malin Landslide, and **b** Satellite view of Malin (taken from Google Map)

4 is steep with an average inclination of 40°. The cross-sectional profile of the Malin slope is shown in Fig. 3. From the reported field observations, the height of the landslide is roughly estimated as 190 m, while the width of the slide varies from 45 to 134 m (Ering et al. 2015). The area affected by landslide is 44,245 m^2, and the length of the slide from

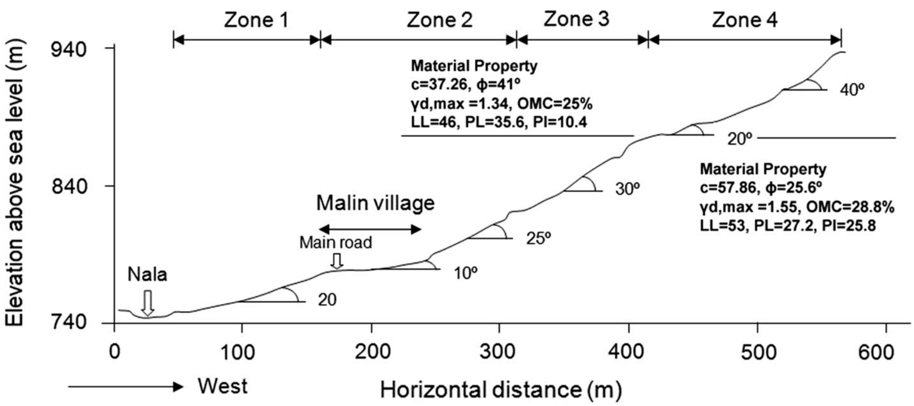

Fig. 3 Cross-sectional profile of the Malin slope

crown to toe is 514 m. The part of Zone 4, entire Zone 3 and the maximum part of Zone 2 were depleted by the landslide. A zone of accumulation was formed by the lowest part of Zone 2 and Zone 1.

Malin area receives 90% of the yearly rainfall during the monsoon season which spans from the month of June to September. The rainfall data just before the 2014 landslide event, that is, from 21 to 30 July 2014 is shown in Fig. 4. It may be observed from the rainfall data that during 22 July to 28 July 2014, there was moderate rainfall, but from 28th July onward, rainfall intensity increased several folds to a maximum on 29th and 30th July with the landslide triggered on early morning of 30 July 2014. So, there is very little doubt about the role of very heavy rainfall in the last 2 days on the triggering of the Malin landslide.

3 Material properties

The material properties of the slide materials and zones above the residential area are obtained from Meshram (2016). Figure 3 shows the material properties of the soils above and below Zone 3 at Malin slope. These data are based on the laboratory tests on the representative soil samples collected from the main slide area and the top of the slope. The grain size distribution curves of the two soil samples collected from main slide area and top of the slope are shown in Fig. 5. The grain size curves indicate that both the soil samples are well graded and silty clay in nature. The density of both the soil samples varies from 1.34 to 1.5 gm/cc, which indicates that not too much variation exists in the soil density. The cohesion of both the soil samples range from 37.26 to 57.86 kPa, with the soil samples collected from the area above the slide has a greater internal friction angle. The engineering properties of the soil samples collected from the slide area and above the slide area are summarised in Table 1.

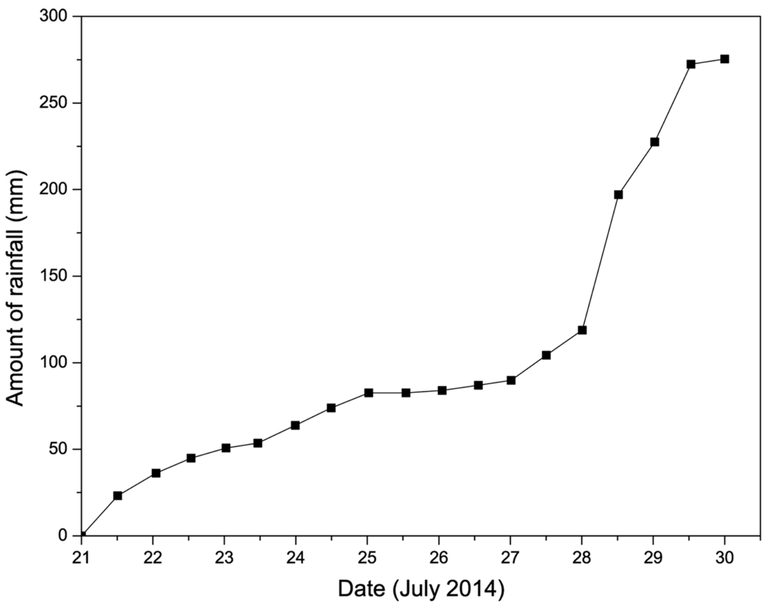

Fig. 4 Rainfall data at Malin before and during the landslide

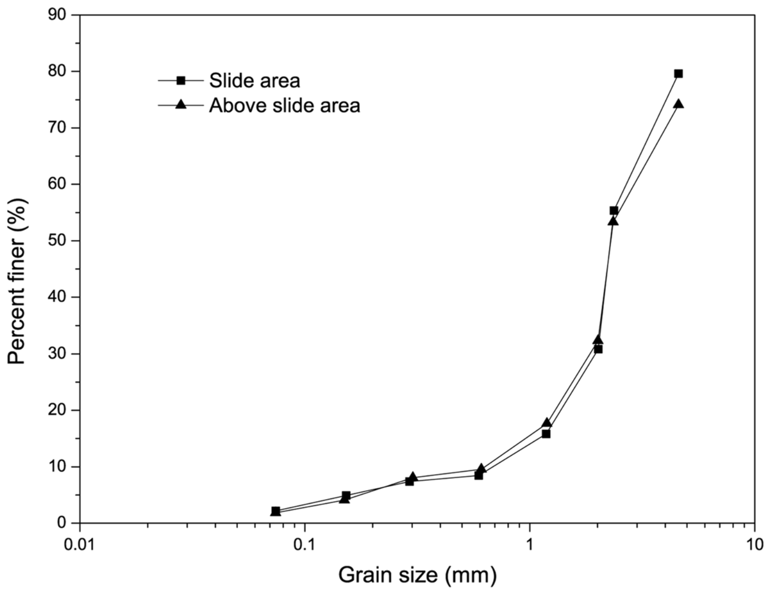

Fig. 5 Grain size distributions of the Malin soils

Table 1 Properties of soil samples

Properties	Slide area	Above slide area
Maximum dry density, $\gamma_{d,max}$ (gm/cc)	1.55	1.34
Optimum moisture content (%)	28.8	25
Liquid limit (%)	53	46
Plastic limit (%)	27.2	35.6
Plasticity Index	25.8	10.4
Shrinkage limit (%)	17.8	17.9
Effective cohesion, c' (kPa)	57.86	37.26
Effective internal friction angle, ϕ' (°)	25.6	41

4 Numerical analyses

In the present study, a commercial software package GeoStudio 2007 (Geo-Slope International Ltd. 2007) is utilised to investigate the effects of the reported rainfall events on the stability of Malin slope. The locations of the ground water level, critical slip surfaces and the corresponding factor of safety of Malin slope under the reported different intensity of rainfall are determined. When the factor of safety becomes less than unity, the slope failure is initiated. It has been reported that the slope above the Malin village (that is, part of Zone 2 and Zone 3) failed, moved downward and gets accumulated on the lower part of Zone 2, unfortunately, this zone of accumulation of debris is the residential area of the Malin village. After the slide happened on 30 July 2014, the local authority removed the debris from the affected area to rescue the survivors. No survey was made on the extent of debris flow, and no DEM of the area are available. For this reason, no attempt has been made to characterise the debris flow in the present study. The present study concentrates on the numerical modelling of the initiation of the instability of Malin slope and on the triggering mechanism with the actual rainfall events.

In the numerical analyses, initially, the hydrological behaviour of the slope is modelled using the SEEP/W program of GeoStudio to determine the seepage, flux and water table within the slope. The SEEP/W program is based on the concept that the fluid flow through both saturated as well as unsaturated soil (Richards 1931; Childs and Collis-George 1950) strictly follows Darcy's law, which states that:

$$q = ki \tag{1a}$$

$$v = ki \tag{1b}$$

where q is the specific discharge per unit area, k is the coefficient of hydraulic conductivity, i is the hydraulic gradient, and v is the Darcian velocity of flow.

The Malin landslide is roughly 190 m in height, 45–134 m in width and 514 m in length, from crown to toe. This entire hill slope is discretised in the numerical analyses (refer to Fig. 6a) by 7132 numbers of two-dimensional 4-noded quadrilateral and 3-noded triangular elements. The initial ground hydrological condition at Malin slope before the rainfall events, which represents the ground conditions at Malin during a moderately dry period, is determined by a steady-state seepage analysis in the SEEP/W program. To be realistic, it is assumed in the numerical analyses that the Malin slope is initially unsaturated. A saturated/unsaturated material model has been adopted for the Malin soils in which a number of functions (hydraulic conductivity function and volumetric water content function) for the Malin hill slope are defined by applying Van Genuchten model (1980) as shown in Fig. 6b. Figure 6b shows the relationship between the hydraulic conductivity and matric suction for both the soil samples, which are developed based on the Van Genuchten model (1980). The figure depicts that with decreasing matric suction, the hydraulic conductivity of the soils increases rapidly, while at the higher matric suction of more than 100 kPa, this variation is not significant.

Van Genuchten (1980) has proposed a relationship to obtain a closed form solution for the hydraulic conductivity function (Eq. 2a) and the volumetric water content function (Eq. 2b), using four parameters.

$$k_{\mathrm{w}} = k_{\mathrm{s}} \frac{\left[1 - \left(a\Psi^{(n-1)}\right)\left(1 + \left(a\Psi^{n}\right)\right)^{-m}\right]^{2}}{\left[\left\{(1 + a\Psi)^{n}\right\}^{\frac{m}{2}}\right]} \tag{2a}$$

where k_{s} is the saturated hydraulic conductivity, a, n and m are the curve fitting parameters, and Ψ is the required suction range. Again, the volumetric water content is related to the residual volumetric water content and the saturated volumetric water content as:

$$\Theta_{\mathrm{w}} = \Theta_{\mathrm{r}} + \frac{\Theta_{\mathrm{s}} - \Theta_{\mathrm{r}}}{\left\{1 + \left(\frac{\Psi}{a}\right)^{n}\right\}^{m}} \tag{2b}$$

where Θ_{w} is the volumetric water content, Θ_{r} is the residual volumetric water content, and Θ_{s} is the saturated volumetric water content. Alternative to the above, a similar type of relationship, as shown below, may be used to develop the volumetric water content function for all the possible negative pressures in the soil between zero and one million kPa, as proposed by Fredlund and Xing (1994).

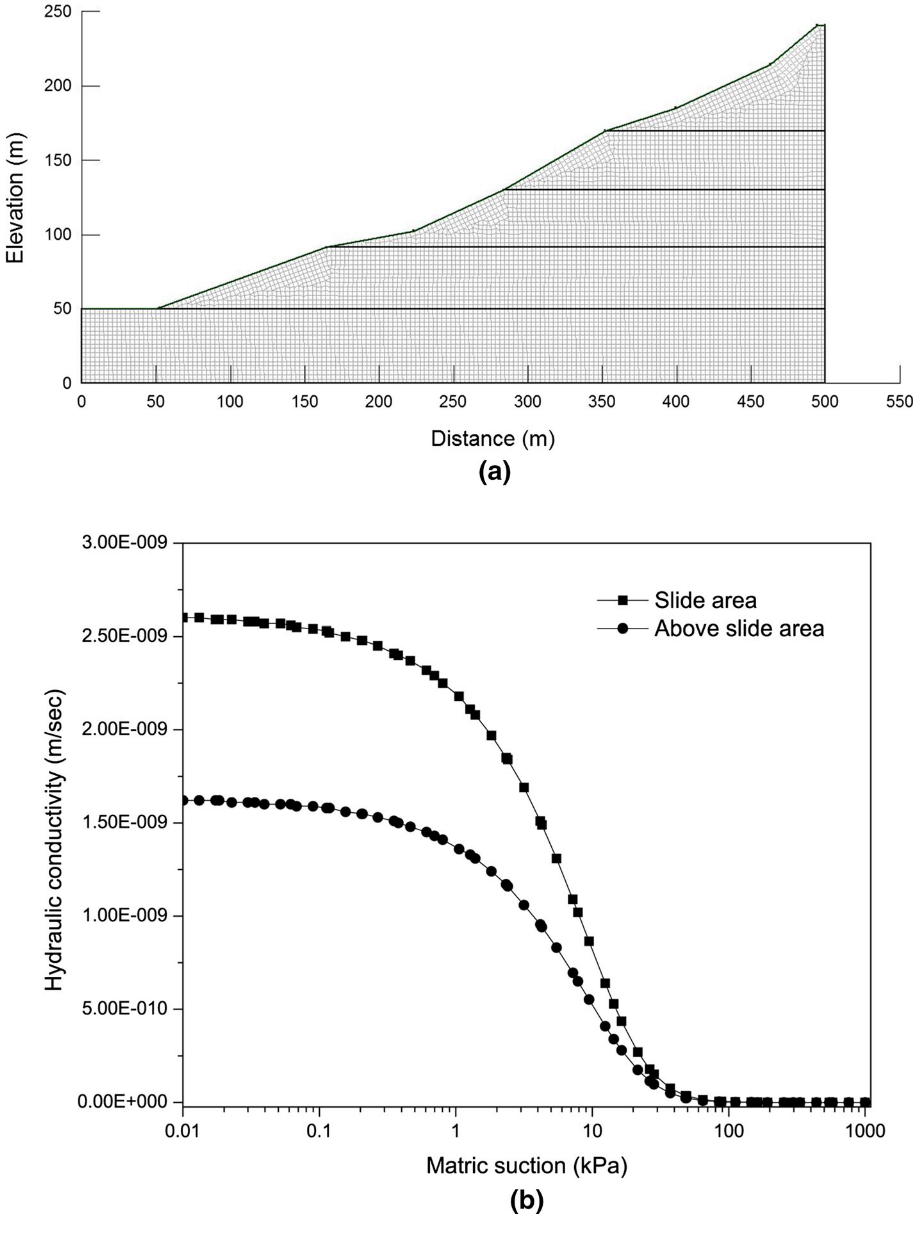

Fig. 6 **a** Discretized model of Malin slope, and **b** hydraulic conductivity function

$$\Theta_{\mathrm{w}} = C_{\Psi} \frac{\Theta_s}{\left\{\ln\left[e + \left(\frac{\Psi}{a}\right)^n\right]\right\}^m} \tag{3}$$

where C_{Ψ} is a correction function.

The Malin village is just 2–3 km from the reservoir of the Dimbhe Dam. A stream or 'nala' (refer to Fig. 3) connected to the Dimbhe Dam reservoir is located at the toe of the Malin hill slope. In the initial steady-state seepage analysis, it is assumed that the base of the hill slope is fully saturated and the hydraulic head is just 1 m above the toe of the slope. The hydraulic head is also specified at the other hill side (vertical) boundary of the slope model. The steady ground water table between these two extreme side boundaries is then obtained by the seepage analysis. This steady ground water condition (as shown in Fig. 7a) represents the location of the initial ground water level in the Malin slope before the rainfall events, that is, before 21 July 2014. The Malin slope above this steady-state ground water table (shown in blue) remains in unsaturated condition with the negative pore water pressures (suction pressures).

The steady-state analysis is followed by transient seepage analyses where the hydraulic condition of the Malin slope is studied due to the rainfall events from 21 July to 30 July

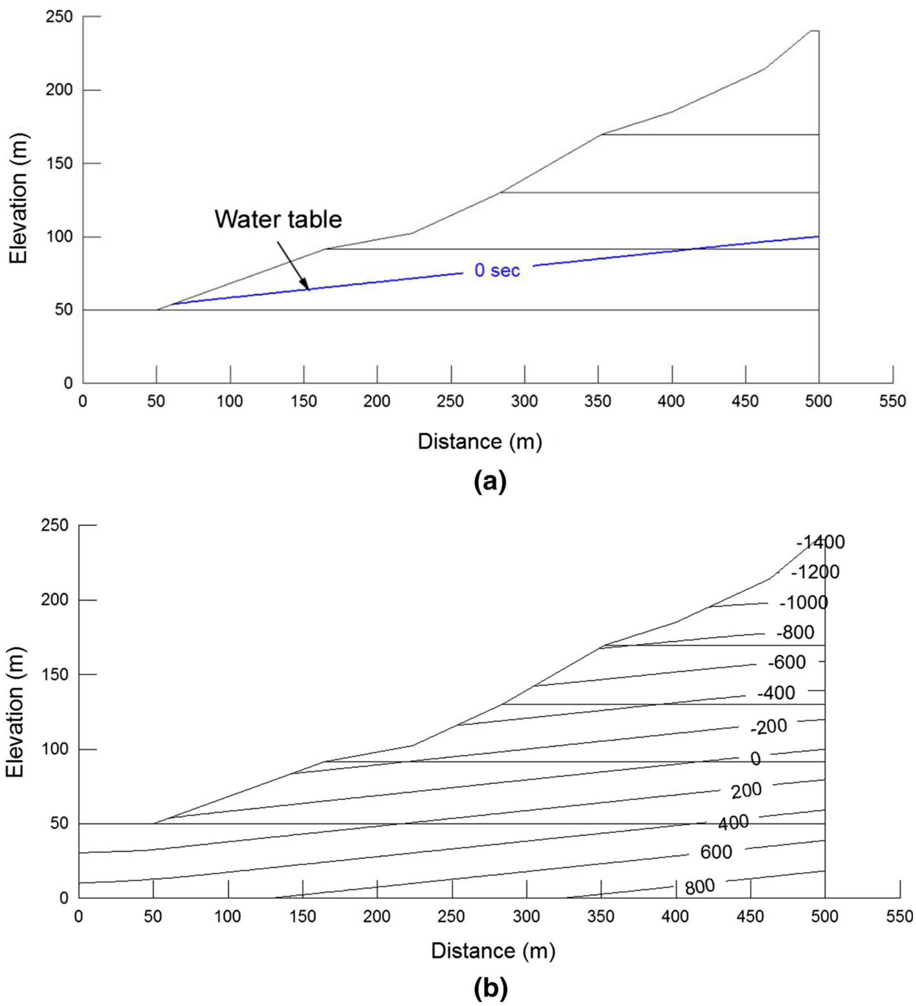

Fig. 7 Initial hydrostatic conditions: **a** water table, and **b** pore water pressure contours

2014 in order to account for the antecedent rainfall on the stability of Malin slope. In the transient seepage analyses, a unit flux as a function of time is applied on the slope surface to simulate the rainfall events. At the beginning, very small flux rates corresponding to the very small intensities of the reported rainfall from 21 July to 28 July 2014 are applied on the horizontal and the inclined surfaces of the slope model and the seepage analyses are performed to obtain the hydraulic conditions of the Malin slope up to 28 July 2014. This is followed by another transient seepage analysis where the actual day to day flux rates are applied on the Malin slope surface corresponding to the devastating rainfall event during 28 July to 30 July 2014. In addition to the above, several transient analyses are also performed as a part of a parametric study, where the ground hydrological effects on the Malin slope are studied for 2 mm/h, 5 mm/h, 10 mm/h, 20 mm/h, 30 mm/h, 40 mm/h, 50 mm/h, 60 mm/h and 70 mm/h intensities of rainfall events, each of 24-h duration. In all the cases, the results are computed for every 1-h interval.

In the seepage analyses, the saturated hydraulic conductivity is a very crucial parameter for the soil as the flux rate directly depends on it. In the present analyses, it is assumed that when the unit flux is greater than the saturated hydraulic conductivity of the soil, a build up of positive pore water pressures within the slope surface will take place until complete saturation and the excess water will runoff over the slope surface.

The SLOPE/W program of GeoSlope is then utilised to calculate the factor of safety of the Malin slope at different time intervals and under different intensity of rainfall events. The SLOPE/W program is formulated based on the concept of the theory of limit equilibrium of moments and forces to determine the safety factor. The theory of limit equilibrium assumes that the safety factor of the cohesive component of the strength and frictional component of the strength remain same for the entire soil mass involved and the factor of safety is same all along the failure or slip surface. In the present analyses, the critical slip surface and the corresponding minimum factor of safety are calculated by three limit equilibrium methods- Bishop's simplified method (1955), Morgenstern–Price method (1965), and Spencer's method (1967). Searches for the most critical (corresponding to minimum factor of safety) circular, non-circular, shallow and deep-seated failure/slip surfaces are made by all the above three limit equilibrium methods. The locations of the most critical slip surface and the corresponding minimum factor of safety obtained by the above three methods are only reported. These three limit equilibrium methods are different depending upon their assumptions regarding the inter-slice forces satisfying the equilibrium conditions. The simplified Bishop's method assumes that the inter-slice forces are horizontal and only satisfies the moment equilibrium condition. The Spencer's method assumes a constant inclination of the inter-slice forces for all the vertical slices. It finds the inter-slice forces and their inclination by iterative process to satisfy both force and moment equilibrium conditions. The Morgenstern and Price (M–P) method of limit equilibrium finds the inter-slice forces and their orientations by satisfying the force and moment equilibrium conditions. In this method, the orientations of the inter-slice forces varying. In the present study, the material model for the soils is assumed to be satisfying Mohr–Coulomb failure criteria with the following modifications for unsaturated condition. The change in viscosity of the soil or that of water within the soil pores and creeping or consolidation behaviours of the soils are not considered in this study. For an unsaturated soil, the soil suction has a direct impact on the shear strength of the soil (Fredlund et al. 1978) and the Mohr–Coulomb's shear strength equation may be rewritten as:

$$S = C' + (\sigma_{\mathrm{n}} - u_{\mathrm{a}}) \tan \phi' + (u_{\mathrm{a}} - u_{\mathrm{w}}) \tan \phi^{b} \tag{4}$$

where S is the shear strength of the unsaturated soil, C' is the effective cohesion, σ_n is the total normal stress, u_a is the pore-air pressure, ϕ' is the effective angle of internal friction, u_w is the pore water pressure, and ϕ^b is an angle defining the increase in the shear strength for an increase in the soil suction. The ϕ^b parameter varies with the degree of saturation. With increasing degree of saturation, this ϕ^b values increases, at 100% saturation this value is equal to the angle of internal friction ϕ. When the soil de-saturates, ϕ^b decreases. Vanapalli et al. (1996) proposed a better alternative to ϕ^b in terms of volumetric water content as shown below:

$$S = C' + (\sigma_n - u_a)\tan\phi' + (u_a - u_w)\left[\left(\frac{\Theta_w - \Theta_r}{\Theta_s - \Theta_r}\right)\tan\phi'\right] \tag{5}$$

where Θ_w is the volumetric water content, Θ_s is the saturated volumetric water content, and Θ_r is the residual volumetric water content. The method proposed by Vanapalli et al. (1996) has been adopted in the present study to model the unsaturated behaviours of the Malin soils. The shear strength parameters for the Malin soils are summarised in Table 1.

In the slope stability analyses, a plane strain condition is assumed. The initial geometry of the slope with the hydrological conditions at the Malin before the rainfall events (that is, before 21st July 2014), during the initial rainfall events, that is, between 21 and 28 July 2014 and during the devastating rainfall events, that is, during 29 to 30 July 2014, are imported from the seepage analyses. The factors of safety of the Malin slope for each case and at each time interval are then calculated. In the slope stability analyses, a potential sliding zone is discretised into a number of vertical slices. Once the resistant and the driving forces are calculated for each of the vertical slices, the factor of safety is then determined by simply integrating the forces over the length of the slip surface. The factor of safety of the assumed sliding surface is defined by Eqs. 6 and 7, which represent the force equilibrium and moment equilibrium, respectively.

$$\mathrm{FS} = \frac{\sum S_r}{\sum S_m} \tag{6}$$

where $\sum S_r$ is the total resistant shear developed and $\sum S_m$ is the total driving shear along the entire length of the slip surface.

$$\mathrm{FS} = \frac{\sum (S_r l_{base})i}{\sum (S_m l_{base})i} \tag{7}$$

where l_{base} is the length of each slice base, and i is the slice index.

5 Results and discussions

The results of the seepage and the slope stability analyses of the Malin slope are presented in terms of variation of pore water pressures, rainfall infiltration, rise of the ground water table, formation of slip surfaces and the corresponding factors of safety against slope failure for the actual rainfall events, and for different rainfall intensities and their duration.

5.1 Initial ground hydrological condition at Malin

The initial hydrological condition existing in the Malin slope as obtained by the initial steady-state seepage analysis is presented in Fig. 7. In Fig. 7b, the ground water table is depicted by the zero pore water pressure contour line. Above the water table, all the pore water pressures in the soil slope are negative and below the water table, all the pressures are positive. At the initial condition, the maximum negative pore water pressure (suction pressure) obtained near the slope surface is about − 1400 kPa. The maximum positive pore water pressure near the bottom most part of the slope is about 800 kPa. The initial hydrological condition depicted by Fig. 7 represents the hydrological condition of Malin slope during a relatively dry state that existed before 21 July 2014. The location of the steady-state water table and the pore water pressures in the slope are mainly controlled by the water level in the stream or discharge from the nearby dam. The corresponding factor of safety of the Malin slope from the slope stability analysis is found to be 1.5. This value is considered to be quite safe against a slope failure. The high value for the factor of safety of the slope is due to the high matric suctions within the soils which apparently increased the shear strengths of the Malin soils.

5.2 Variation of the volumetric water content and matric suction within the Malin soils and factors of safety of Malin slope during actual rainfall events

The average depth of the soil mass moved in Malin cannot be determined accurately, as the field mapping work was carried out, after the removal of most of the debris. However, it is estimated (Ering et al. 2015; Meshram 2016) that the depth of the sliding mass varied from 2 m to a maximum of 7 m. In this study, an average depth of 5 m has been chosen for the potential sliding mass to get an idea about the water content and matric suction variation on the sliding mass with the intensity and duration of rainfall. Figure 8a shows the variation of volumetric water content at a depth of 5 m and 2 m below the slope surface for the actual rainfall events at Malin. As observed from the figure, the volumetric water content at 2 m depth increases significantly with the continuation of rainfall. However, it remains less affected at 5 m depth.

Figure 8b shows the variation of matric suctions in Malin soils at 2 m and 5 m below the slope due to the actual rainfall events. It may be observed from Fig. 8b, in case of actual rainfall data of Malin, the matric suction more or less remains constant at the 5 m depth, while it is decreasing rapidly at 2 m depth. This result indicates possibility of a shallow type of landslide at Malin.

It may be also observed that the variation of pore water pressures, volumetric water contents and matric suctions at the Malin slope with the duration of rainfall is not too high, because of the slope materials (silty clay), whose coefficient of permeability (hydraulic conductivity) is quite low to allow percolation of rainwater quickly through the soil mass.

Figure 9a shows the variation of the factor of safety (from Bishop, M–P and Spencer methods) with the duration of the actual rainfall at Malin from 21 July 2014 to 30 July 2014, and the corresponding minimum factors of safety (FOS) against sliding failure of the Malin slope (refer to Table 2). The rainfall data at Malin are reported at 24-h interval. To estimate the intensity of the rainfall, the rainfall data have been divided by 24 h assuming the rainfall intensity to be uniform throughout the day. The results indicate that, on 21 July 2014, before the continuous rainfall events, the factor of safety of the Malin slope is 1.492, which is more than adequate. After 2 days of small intensities of rainfall, the factor of safety of the Malin slope remain unchanged, it varies from 1.492 to 1.498. From 24 July 2014, the factor of safety reduces rapidly and becomes 1.266 on 25 July 2014. After 25 July 2014, the rainfall reduced or stopped and the factor of safety increases again to 1.422.

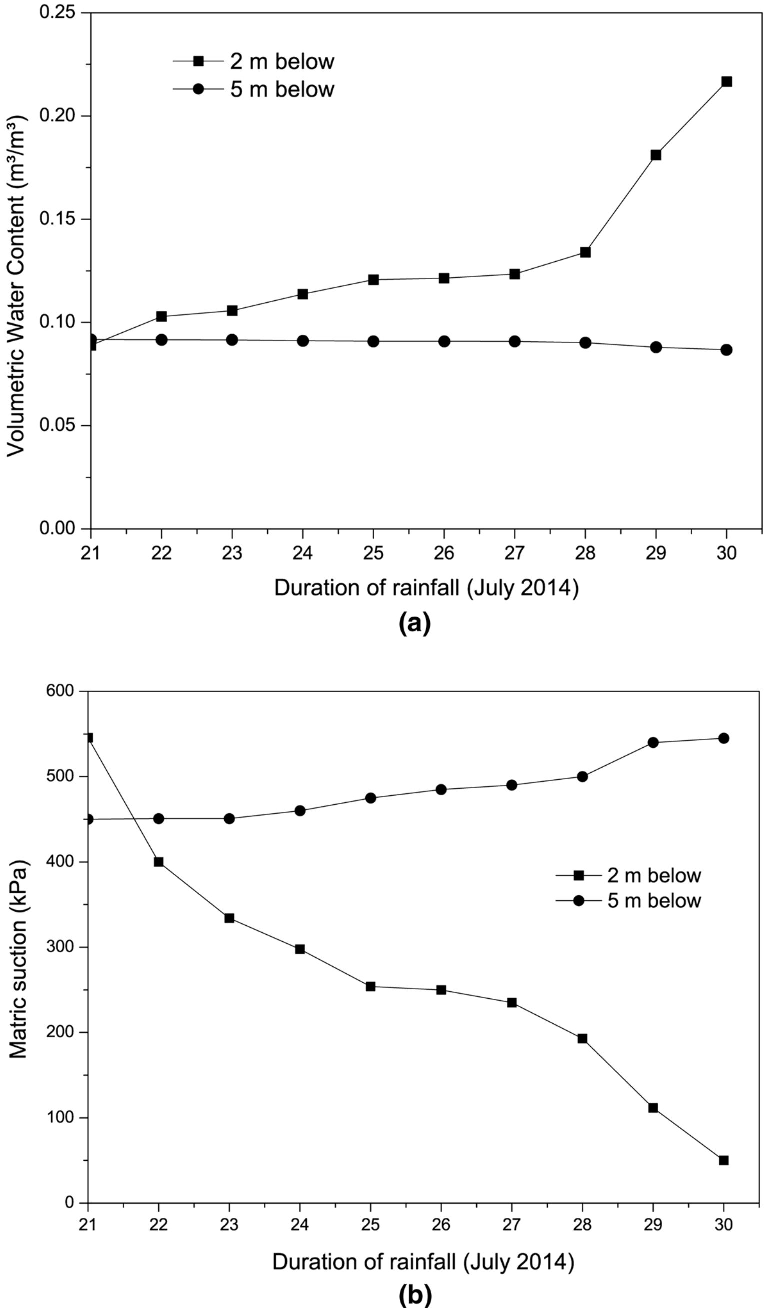

Fig. 8 **a** Variation of volumetric water content, and **b** variation of matric suction with the duration of rainfall at 5 and 2 m below the Malin slope surface under the actual rainfall at Malin

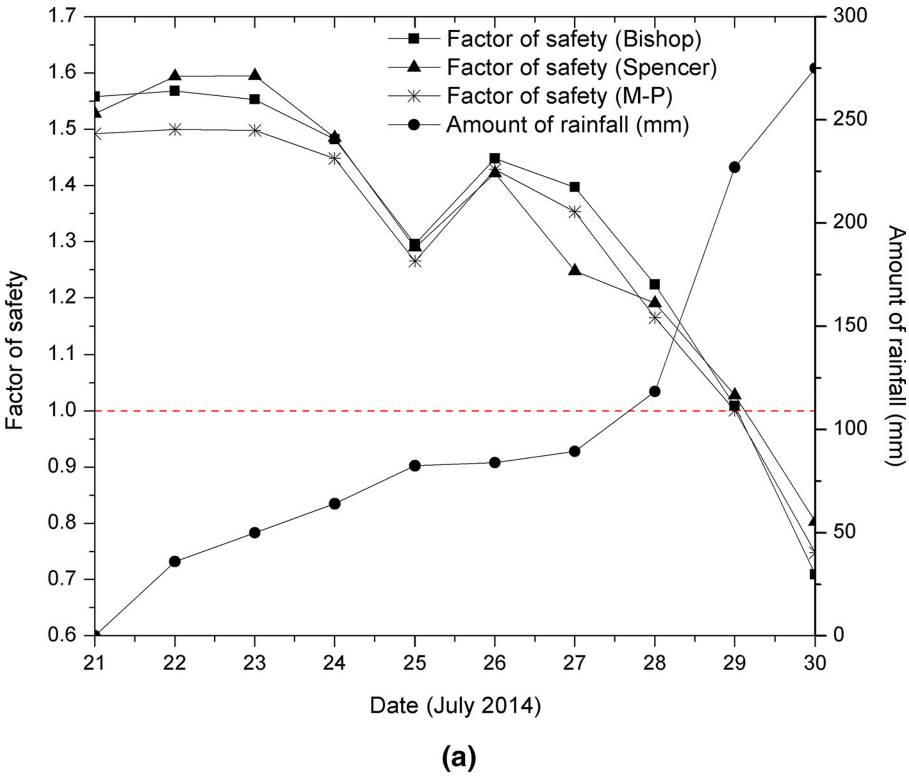

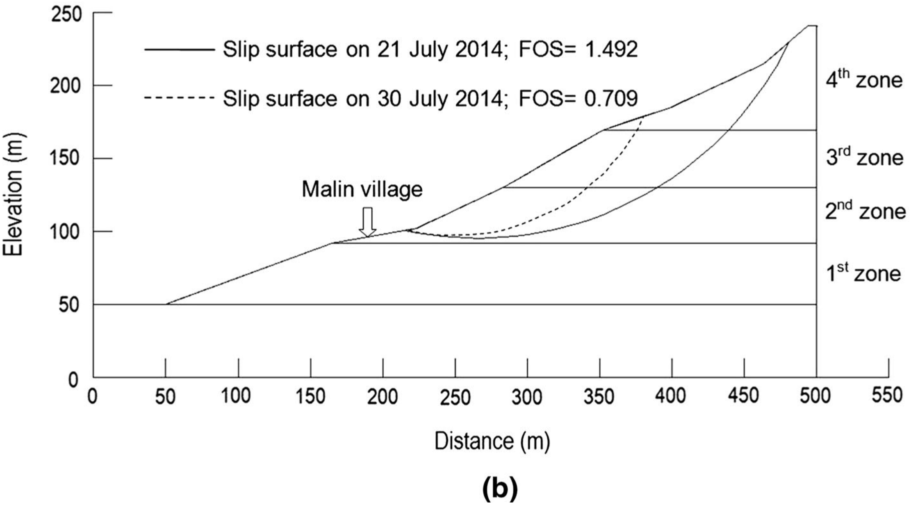

Fig. 9 **a** Variation in the factor of safety with the duration of rainfall from 21 July, 2014 at Malin, and **b** critical slip surfaces at Malin slope before rainfall (21 July 2014) and on the day of tragedy (30 July 2014)

Table 2 Minimum FOS obtained from 21 July 2014 to 30 July 2014, at Malin

Day (July, 2014)	FOS
21	1.492
22	1.500
23	1.498
24	1.448
25	1.266
26	1.422
27	1.248
28	1.165
29	1.001
30	0.709

From 27 July 2014, heavy rainfall commenced and the factor of safety reduces rapidly. After 29 July 2014, the factor of safety of Malin slope becomes less than one and the slope failure takes place. This matches with the reported landslide at Malin.

Figure 9b shows the location of the critical slip surfaces on 21 July 2014 and on 30 July 2014. The location of the failure surface corresponding to the 30 July 2014 confirms that the slope, (lower part of the Zone 2) on which the Malin village is located, is safe but not fully secured because of the failure of the upslope of the Malin village (upper part of the Zone 2 and Zone 3). The failed soil mass moves from the Zone 3 in the downward direction and accumulated on the lower part of the Zone 2. Unfortunately, this zone of accumulation of debris is the residential area of the Malin village. Thus, the present numerical analyses have been able to model the failure sequence of the Malin slope and the destruction of the Malin village quite accurately.

5.3 Water table variation and its effects on the slope stability during rainfall

The behaviour of the ground water table within the Malin slope is obtained under the different hypothetical intensity of rainfall by calculating the infiltration rate of rain water through the Malin soil slope. At the beginning of the rainfall infiltration in Malin slope, for each case, a perched water table is found to develop in addition to the permanent ground water table at a depth as shown in Fig. 10a, c. The temporary perched water table is developed due to the rainfall infiltration. The initially unsaturated ground becomes saturated as the infiltrated rain water moves in the downward direction due to gravity. With the increase in the duration of rainfall, the permanent ground water table moves in the upward direction very slowly, while the perched water table moves rapidly downward, towards the permanent ground water table. This movement of perched water table becomes faster with the increase in the intensity of rainfall. The results for two different rainfall intensities are compared to have an idea about the movement of the ground water table with time (isolines) and to demonstrate how deep the perched water table can move for a specified rainfall duration. A normal intensity of rainfall of 20 mm/h and a high rainfall intensity of 60 mm/h have been chosen for this study. Figure 10b shows the isolines for 20 mm/h of rainfall, where the perched water table has moved to an average depth of 3.5 m in 24 h. Figure 10d shows the isolines for 60 mm/h of rainfall. In this case, the perched water table has moved to an average depth of 7.1 m in 24 h. From the literature (Ering et al. 2015; Meshram 2016), it has been found that the average thickness of the sliding mass

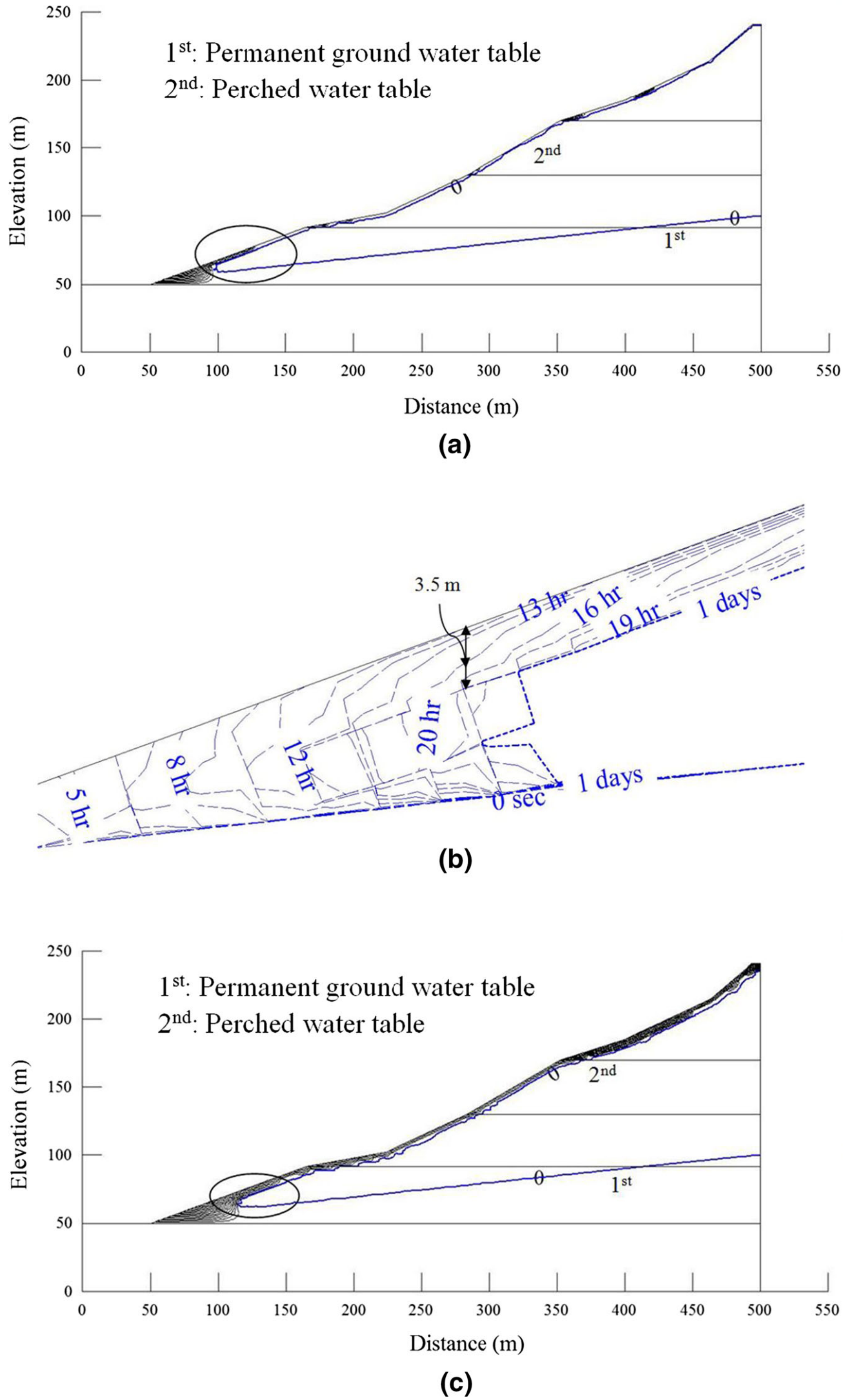
1st: Permanent ground water table
2nd: Perched water table
Elevation (m)
Distance (m)
0
50
100
150
200
250
300
350
400
450
500
550
2nd
1st
0
(a)
3.5 m
5 hr
8 hr
12 hr
13 hr
16 hr
19 hr
20 hr
1 days
0 sec
1 days
(b)
1st: Permanent ground water table
2nd: Perched water table
Elevation (m)
Distance (m)
2nd
1st
0
(c)

◀ **Fig. 10** Movement of the ground water tables with respect to the duration of rainfall: **a** water table for 20 mm/h rainfall after 24 h, **b** magnified view of isolines of the marked portion of the above figure **a**, **c** water table for 60 mm/h rainfall after 24 h, and **d** magnified view of isolines of the marked portion of the above figure **c**

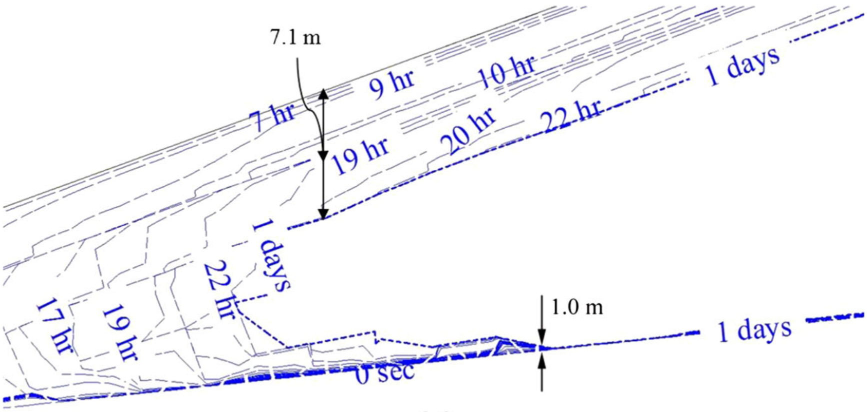

Fig. 10 continued

during rainfall-induced slope failure varies from 2 to 7 m. Thus, the perched water table has a direct impact on the stability of the Malin slope. As the depth of the perched water table increases with the duration and the intensity of rainfall, the positive pore water pressures within the ground increase and the soil suction pressures along with the shear strengths of the top soil layers reduce leading to a slope failure. It may be also observed that the movement of the permanent ground water table is only about 1 m between the two cases considered, which is actually much less compared to the movement of the perched water table and it does not have any significant role or effect on the stability of the Malin slope.

5.4 Pore water pressure, water content and matric suction variation with the duration of a 10 mm/h rainfall event

Figure 11a shows the predicted pore water pressure distribution along the potential slip (failure) surfaces for a rainfall intensity of 10 mm/h The figure depicts that the pore water pressures along the slip surfaces increase and the corresponding factor of safety of the slope reduces with the increase in the duration of the rainfall. After 1 h of rainfall, the factor of safety of the Malin slope is 1.476. It further reduces to 1.092 after 24 h of rainfall. At the beginning of the rainfall event, the slip surface is above or very close to the water table and the pore pressures in the soil are negative or very close to zero. But with the increasing rainfall duration, the slip surfaces extend below the water table and the pore water pressures in the soil become positive. Figure 11b shows some of the corresponding slip surfaces for 10 mm/h of rainfall.

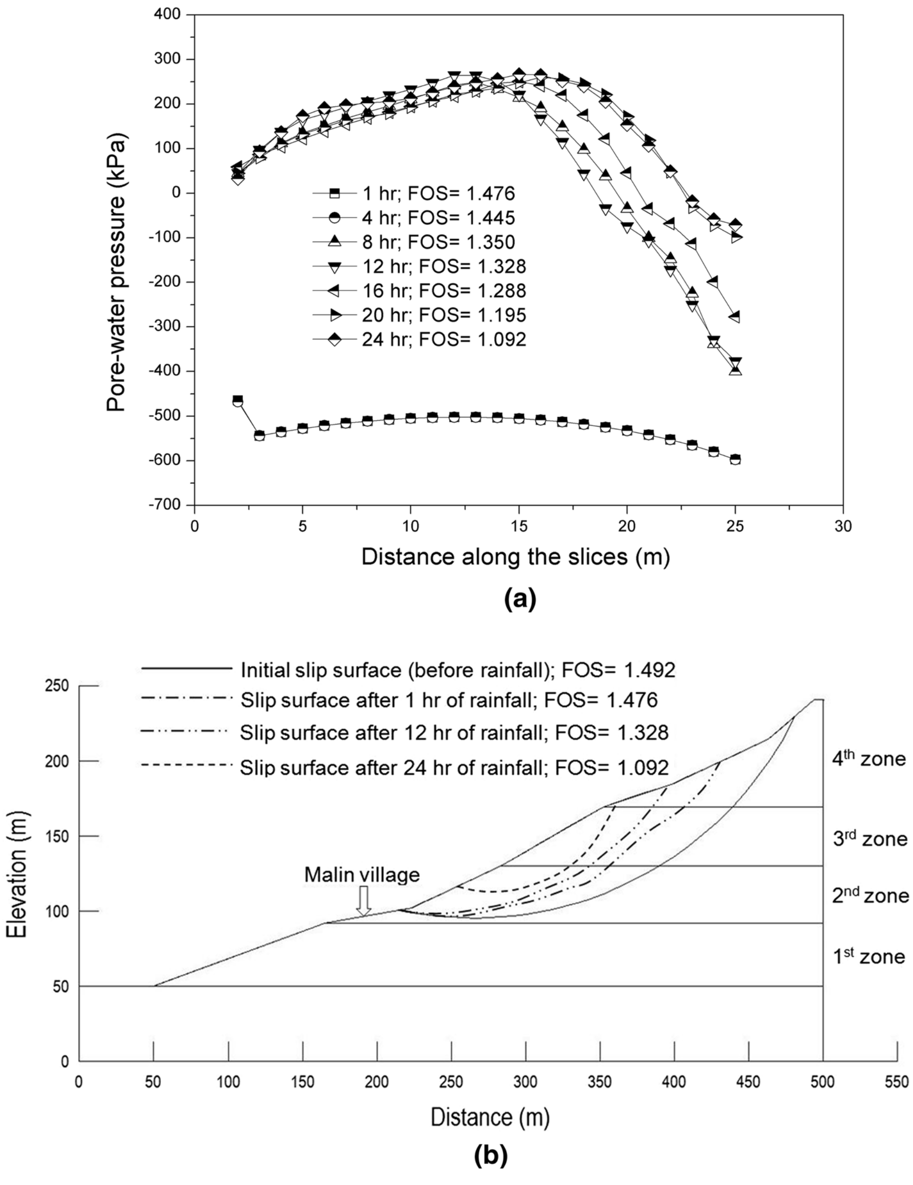

Fig. 11 **a** Pore water pressures, and **b** corresponding slip surfaces for 10 mm/h of rainfall

5.5 Variation of the factor of safety of Malin slope with the intensity and the duration of the rainfall

In this study, as before, an average depth of 5 m has been chosen for the potential sliding mass to get an idea about the water content and matric suction variation on the sliding mass with the duration of different hypothetical intensity of rainfall. Figure 12a shows the variation of volumetric water content at a depth of 5 m below the slope surface for the

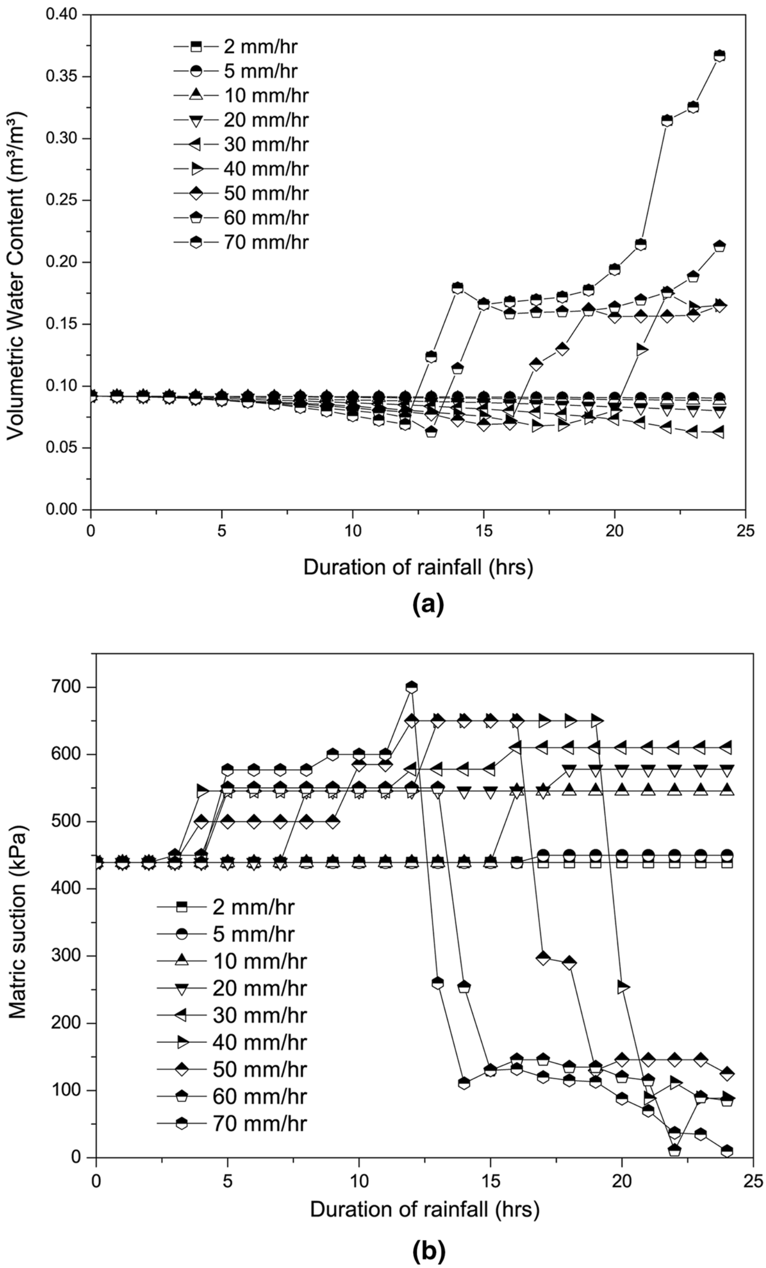

Fig. 12 **a** Variation of volumetric water content, and **b** variation of matric suction at a depth of 5 m below the surface under different intensity of rainfall

different intensity of rainfall. It may be observed that the lower intensity rainfalls, such as 2, 5, 10, 20 and 30 mm/h, do not have any significant influence at a depth of 5 m, while the higher intensity rainfalls have a significant effect at this depth. It may be also observed that at 5 m depth, initially the water content decreases with time. During the transient seepage, the percolation of rainwater into the ground takes some time and in the case of lower intensity rainfall, the rainwater takes longer time to percolate to the 5 m depth and thus the water content decreases and the matric suction increases temporarily at this depth. On the other hand, in case of higher intensity of rainfall, such as 40, 50, 60 and 70 mm/h, the volumetric water content at 5 m depth increases rapidly.

Figure 12b shows the matric suction variation with the duration of different intensity of rainfall at a depth of 5 m below the slope surface. It may be seen from the figure that the lower intensity rainfalls, such as 2, 5, 10, 20 and 30 mm/h, do not have any influence at a depth of 5 m, while the higher intensity rainfalls have a significant effect at this depth.

The minimum factor of safety against sliding of the Malin slope is calculated at each of the time steps (at every 1-h interval) during the 24-h rainfall events for all the rainfall intensities (2 mm/h, 5 mm/h, 10 mm/h, 20 mm/h, 30 mm/h, 40 mm/h, 50 mm/h, 60 mm/h and 70 mm/h) and shown in Fig. 13. At the low intensities of rainfall, the factors of safety do not vary significantly, however at higher intensities of rainfall, the factors of safety drop rapidly with the duration of rainfall. It may be noticed from Fig. 13 that, in the case of 2 mm/h, 5 mm/h and 10 mm/h of rainfall, the stability of the Malin slope is adequate (greater than 1) even after 24 h of continuous rainfall. The factor of safety drops to 1.092 in the case of 10 mm/h rainfall after 24 h, while the stability more or less remains constant in the case of 2 mm/h and 5 mm/h of rainfall. On the other hand, the factor of safety of the Malin slope drops rapidly in the cases of 20 mm/h, 30 mm/h, 40 mm/h, 50 mm/h, 60 mm/h and 70 mm/h of rainfall intensities and become unstable after 7, 6, 6, 3, 2 and 1-h, respectively. As the higher intensity and the longer duration of rainfall allow the rainwater to infiltrate to a greater depth, it reduces the soil suction and the shear strength for a large mass of soil which triggered the slope failure. In this context, the following observations may be made based on the present analyses: (1) A continuous rainfall of 20 mm/h for more than 7 h is not impossible at the Malin area because this place is very close to Mumbai and

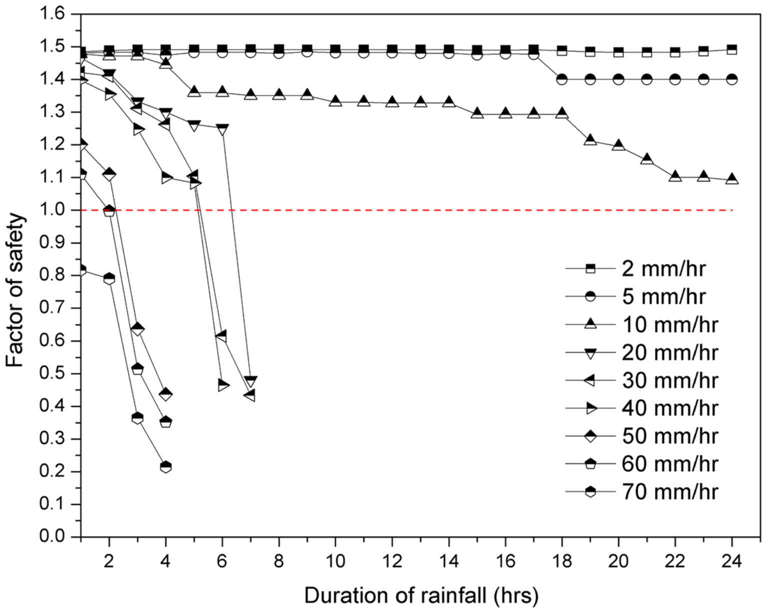

Fig. 13 Reduction of factor of safety with the increasing intensity and the duration of rainfall

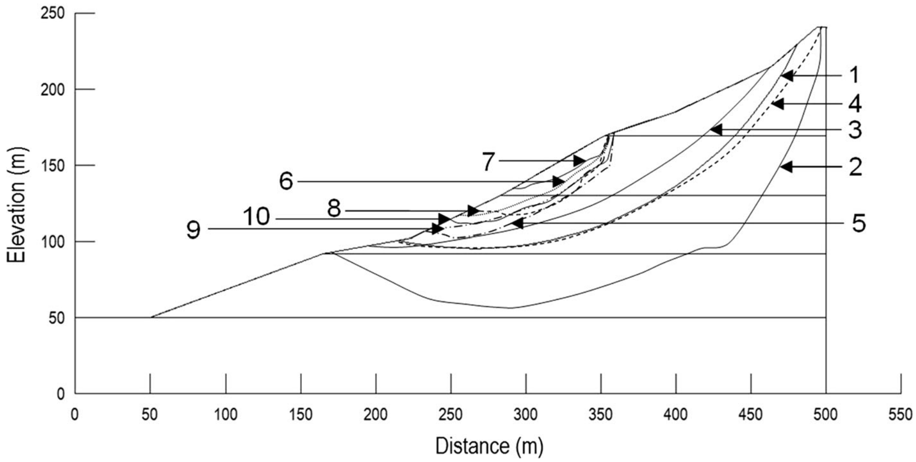

Fig. 14 Critical slip surfaces at Malin slope under different intensities of rainfall

according to the intensity duration frequency (IDF) curves of Mumbai city, it can happen once in every 2 years (Zope et al. 2016). (2) For a continues rainfall of 70 mm/h, the factor safety reduces after 1 h to 0.817; thus, the slope becomes unstable and according to IDF curves, such intensity and duration of rainfall can happen once in every 5 years. Thus, the intermediate rainfall intensity such as 30 mm/h, 40 mm/h, 50 mm/h and 60 mm/h can make the Malin slope unstable within 6, 6, 3 and 2 h, respectively.

Figure 14 shows the critical slip surfaces within the Malin slope for nine different intensities of rainfall considered. For the ten cases presented in Fig. 14 and the corresponding minimum FOS against sliding failure of the Malin slope (refer to Table 3).

From the above parametric study, it is observed that for 24 h of 10 mm/h or less intensity of rainfall, Malin slope is not failing. But for 20 mm/h or higher intensity of rainfall, the Malin slope will fail within 24-h. duration. For the higher intensities (greater than 10 mm/h) of rainfall, it has been found that the Malin slope will fail with the slip surfaces going through the upper part of Zone 2 to Zone 3. As in the actual case, the failed soil mass may move from the Zone 3 in the downward direction and potentially destroy the residential area of the Malin village.

6 Conclusions

A highly destructive rainfall-induced slope failure at Malin near Mumbai, India, has been investigated numerically and the day-by-day situation leading up to the failure of the Malin slope has been recreated. The following conclusions are drawn from the results of this study.

1. The numerical study indicates that the continuous rainfall infiltration develops a perched water table near the slope surface at Malin. As a result, the surface materials remain saturated and the positive pore water pressures develop at shallow depths. With the increasing intensity and duration of rainfall, the depth of this saturated zone increases rapidly. However, the movement of the permanent ground water table at depth is found to be not significant and does not have any notable effect on the stability of the Malin slope.

Table 3 Different intensities of rainfall considered and the corresponding FOS against sliding of Malin slope

Slip surface	Case	FOS
1	Initial slip surface (before rainfall)	1.492
2	2 mm/h rainfall after 24 h	1.490
3	5 mm/h rainfall after 24 h	1.400
4	10 mm/h rainfall after 24 h	1.092
5	20 mm/h rainfall after 7 h	0.481
6	30 mm/h rainfall after 6 h	0.614
7	40 mm/h rainfall after 6 h	0.445
8	50 mm/h rainfall after 3 h	0.637
9	60 mm/h rainfall after 2 h	0.997
10	70 mm/h rainfall after 1 h	0.817

2. The numerical results demonstrate a significant effect of the pore water pressures and soil suction pressures on the stability of the Malin slope. With the rainfall infiltration into the ground, the suction pressures in the soil decrease, the pore water pressures become positive and thus the shear strengths of the slope material reduces and the factor of safety against sliding also reduces.
3. The parametric study indicates that, in the cases of 2 mm/h, 5 mm/h and 10 mm/h of rainfall, the factor of safety of the Malin slope is adequate even after 24 h of continuous rainfall. In the cases of 20 mm/h, 30 mm/h, 40 mm/h, 50 mm/h, 60 mm/h and 70 mm/h of rainfall, the factor of safety of the Malin slope drops rapidly and becomes unstable after 7, 6, 6, 3, 2 and 1 h, respectively.
4. It is observed that the Malin slope is able to resist a 60 mm/h of rainfall for a duration of almost 2 h, this is because of the slope materials (silty clay), whose coefficient of permeability (hydraulic conductivity) is low enough not to allow the rainwater percolate through the soil mass quickly. As a result, the positive pore water pressures within the slope do not increase rapidly at depth and the excess rain water moves along the slope surface as a surface runoff. On the other side, the same reason makes the Malin slope more risky, as because of the low coefficient of permeability, the rainwater infiltrating into the ground with time cannot drain out easily, which is causing an increase in the positive pore water pressures and reduction in the factor of safety.
5. From the actual day-by-day analyses of Malin slope failure, it is observed that the initially stable Malin slope becomes weaker with rainfall duration. On 21 July 2014 before the rainfall, the minimum factor of safety against sliding is 1.6. But as the time progresses, this minimum factor of safety reduces and becomes less than one on 30th July 2014, the day of tragedy.
6. From the numerical analyses, it has been observed that the Malin slope (lower part of the Zone 2) on which the Malin village is located is safe but not entirely secured because of the failure of the upslope (upper part of Zone 2 and Zone 3) of the Malin village. The failed soil mass would move from upper part of Zone 2 and Zone 3 in the downward direction and destroy the Malin village located on the lower portion of Zone 2.

References

BBC News (30 July 2014) http://www.bbc.com/news/world-asia-28559617. Accessed 20 June 2017
Bishop AW (1955) The use of the slip circle in the stability analysis of slopes. Geotechnique 5(1):7–17
Bishop AW (1959) The effective stress principle. Teknisk Ukeblad 39:859–863
Borja RI, White JA (2010) Continuum deformation and stability analyses of a steep hillside slope under rainfall infiltration. Acta Geotech 5(1):1–14
Brown III WM, Sitar N, Saarinen TF, Blair M (1982) Overview and summary of debris flows, landslides, and floods in the San Francisco Bay region, January 1982. In: Conference on debris flows, landslides, and floods in the San Francisco Bay region, Stanford University, Stanford, CA, USA, pp 1–66
Childs EC, Collis-George N (1950) The permeability of porous materials. Proc R Soc 201(1066):392–405
Ering P, Kulkarni R, Kolekar Y, Dasaka SM, Babu GS (2015) Forensic analysis of Malin landslide in India. In: IOP conference series: earth and environmental science, vol 26, no 1. IOP Publishing, p 012040
Fredlund DG, Rahardjo H (1993) Soil mechanics for unsaturated soils. John, New York
Fredlund DG, Xing A (1994) Equations for the soil-water characteristic curve. Can Geotech J 31(4):521–532
Fredlund DG, Morgenstern NR, Widger RA (1978) The shear strength of unsaturated soils. Can Geotech J 15(3):313–321
GEO-SLOPE International Ltd (2007) GeoStudio. Calgary, Alberta, Canada
Lagmay AMF, Ong JBT, Fernandez DFD, Lapus MR, Rodolfo RS, Tengonciang AMP, Soria JLA, Baliatan EG, Quimba ZL, Uichanco E, Paguican A (2006) Scientists investigate recent Philippine landslide. Am Geophys Union 87(12):121–128
Meshram S (2016) Investigations of the causes of landslide at Malin and some preventive measures. J Geotech Stud 1(2):1–14
Morgenstern NR, Eo Price V (1965) The analysis of the stability of general slip surfaces. Geotechnique 15(1):79–93
Naithani AK (1999) The Himalayan landslides. Employ News 23(47):1–2
Naykodi A, Takalkar O, Bhor A, Jadav K, SA N (2016) A review paper on slope stability analysis of Malin landslide. In: TECHNOPHILIA-2016, Jaihind Polytechnic, Kuran, India, pp 101–106
Rahardjo H, Lim TT, Chang MF, Fredlund DG (1995) Shear-strength characteristics of a residual soil. Can Geotech J 32(1):60–77
Richards LA (1931) Capillary conduction of liquids through porous mediums. J Appl Phys 1(5):318–333
Schuster RL, Salcedo DA, Valenzuela L (2002) Overview of catastrophic landslides of South America in the twentieth century. Rev Eng Geol 15:1–34
Sengupta A, Gupta S, Anbarasu K (2010) Rainfall thresholds for the initiation of landslide at Lanta Khola in north Sikkim, India. Nat Hazards 52:31–42
Spencer E (1967) A method of analysis of the stability of embankments assuming parallel inter-slice forces. Geotechnique 17(1):11–26
Van Genuchten MT (1980) A closed-form equation for predicting the hydraulic conductivity of unsaturated soils. Soil Sci Soc Am J 44(5):892–898
Van Sint Jan M, Talloni P (1993) Flujo de sedimentos del 18 de Juniode 1991 en Antofagosta: La Serena, Chile. In Tercer Congreso Chileno de Ingenieria Geotecnia 1:247–265
Vanapalli SK, Fredlund DG, Pufahl DE, Clifton AW (1996) Model for the prediction of shear strength with respect to soil suction. Can Geotech J 33(3):379–392
Wilson CJ, Dietrich WE (1987) The contribution of bedrock groundwater flow to storm runoff and high pore pressure development in hollows. IAHS AISH Publ 165:49–59
Zope PE, Eldho TI, Jothiprakash V (2016) Development of rainfall intensity duration frequency curves for Mumbai City, India. J Water Resour Prot 8(7):756–765